This article has been accepted for publication in a future issue of this journal, but has not been fully edited. Content may change prior to final publication. Citation information: DOI 10.1109/LCOMM.2021.3085399, IEEE Communications Letters

Multi-User Interference Cancellation for Uplink FBMC-based Multiple Access Channel

Sumaila Mahama, *Student Member, IEEE*, Yahya J. Harbi, *Member, IEEE*, David Grace, *Senior Member, IEEE*, and Alister G. Burr, *Senior Member, IEEE*

***Abstract*—In the uplink of multi-user systems, signals from different users may arrive at the base station with different timing offsets (TO), which degrades the performance of conventional OFDM systems. In this letter, an FBMC-based multiple access channel with timing errors is considered under frequency selective channels. To eliminate the intrinsic interference (InI), TO-induced interference (TOI) and multi-user interference (MUI) terms, an iterative receiver is proposed. The proposed receiver combines bit-interleaved coded modulation with iterative decoding (BICM-ID) processing with parallel interference cancellation and iterative interference cancellation. The results show that FBMC is robust to timing errors and the proposed receiver can effectively eliminate the interference terms. This motivates the use of FBMC as an alternative to OFDM in applications that require asynchronous transmissions.**

***Index Terms*—FBMC-QAM, OFDM, asynchronous access, interference cancellation, LDPC, BICM-ID.**

I. Introduction

WIRELESS networks beyond 5G are expected to handle the coexistence of many use cases, including massive machine-type communications (mMTC). To connect to the network each user equipment (UE) performs an uplink synchronization procedure by sending a scheduling request to the base station (BS) and waiting for the BS to grant it radio resources [1]. For some mMTC applications, this grant-based multiple access will result in a huge synchronization overhead, due to the high connection density. To solve this problem, grant-free transmission has been investigated for mMTC, in which each UE operates in a wake-up-and-transmit manner [1]. However, in a grant-free system there is timing misalignment of UE transmissions which introduces asynchronous interference [2].

Orthogonal frequency division multiplexing (OFDM), which has been adopted for LTE and 5G New Radio (NR), requires the grant-based synchronization procedure in order to maintain orthogonality between subcarriers. In addition, OFDM suffers from poor spectrum containment which makes it sensitive to timing errors. This makes OFDM inefficient for the relaxed synchronization required in the grant-free uplink transmission of mMTC devices [3]. Recently, non-orthogonal waveforms have been shown to be robust to imperfect synchronization [4], [5]. In [1], an uplink asynchronous multi-user system with generalized frequency division multiplexing (GFDM) was investigated and a weighted parallel interference cancellation (PIC) receiver was proposed to cancel the multi-user interference (MUI).

Another waveform candidate that has shown robustness in asynchronous scenarios is filter-bank multicarrier (FBMC) [6], which employs per subcarrier filtering using well-localized filters. As a result, FBMC exhibits significantly lower out-of-band (OOB) emissions compared to both OFDM and GFDM. In addition, FBMC systems require no cyclic prefix (CP) and guard band, which can significantly improve spectral efficiency. However, the orthogonality between sub-channels is lost, resulting in intrinsic interference (InI). An implementation of FBMC that has received significant research attention is the FBMC with offset quadrature amplitude modulation (FBMC-OQAM) [7], [8]. In [7], the performance of FBMC-OQAM in a multi-user massive multiple-input multiple-output (MIMO) systems is investigated by exploiting the statistical properties of the InI in FBMC-OQAM. The authors in [8] analysed the interference power in an uplink asynchronous system employing FBMC-OQAM and showed that FBMC-OQAM outperforms OFDM in asynchronous scenarios. However, FBMC-OQAM systems achieve orthogonality only in the real domain and suffer from InI in complex fading channels. Thus, the OQAM processing limits the direct application of FBMC-OQAM in conventional receiver processing such as channel estimation, space-time block coding (STBC) and maximum likelihood detection (MLD). Moreover, [8] only presented a distortion analysis and did not propose a scheme to cancel the InI and MUI terms.

In this letter, a novel interference cancellation receiver is proposed for asynchronous multi-user uplink FBMC-based systems. To resolve the problems with OQAM processing, FBMC with QAM modulation is implemented [3]. The proposed receiver uses bit-interleaved coded modulation with iterative decoding (BICM-ID) which combines FBMC demodulation and SISO decoding for signal detection, and PIC and iterative interference cancellation (IIC) for interference removal [9]. In the initial decoding iteration, each UE's transmit signal is estimated and used to cancel MUI in the PIC phase. In the subsequent decoding iterations, IIC is used to cancel the InI and TO-induced interference (TOI) in each UE's received signal. This differs fundamentally from the GFDM system in [1], which employs a linear adaptive interference cancellation filter to effectively remove the InI terms.

This work was supported by the European Union's Horizon 2020 programme under grant 722788 (SPOTLIGHT project).

Sumaila Mahama, David Grace, and Alister G. Burr are with the Department of Electronic Engineering, University of York, York, United Kingdom (email: sumaila.mahama@york.ac.uk; david.grace@york.ac.uk; alister.burr@york.ac.uk).

Yahya J. Harbi is with the University of Kufa, Najaf, Iraq (email: yahyaj.harbi@uokufa.edu.iq).

Corresponding author: Sumaila Mahama (sumaila.mahama@york.ac.uk).

This article has been accepted for publication in a future issue of this journal, but has not been fully edited. Content may change prior to final publication. Citation information: DOI 10.1109/LCOMM.2021.3085399, IEEE Communications Letters

The rest of the paper is organized as follows: Section II-A, II-B and II-C present the transmitter model, received signal with no TO and received signal with TO, respectively, for the FBMC-based multiple access channel. In Section II-D, a BICM-ID receiver with interference cancellation is proposed to cancel the InI, TOI and MUI in the multi-user FBMC-QAM system. Simulation results are presented in Section III to illustrate the performance of the proposed receiver for both FBMC-QAM and OFDM. Finally, concluding remarks are drawn in Section IV.

Notation: Lower and upper case boldfaces are used to denote vectors and matrices, respectively. $\mathbf{A}(i_1 : i_2, l_1 : l_2)$ represents the submatrix of matrix $\mathbf{A}$ with rows i_1 through i_2 and columns l_1 through l_2 removed. Also, $\mathbb{E}[\cdot]$ represents the expectation operation and $j = \sqrt{-1}$. $\mathbf{I}_P$, $\mathbf{0}_P$ and $\mathbf{0}_{p\times q}$ denote the $P \times P$ identity matrix, $P \times P$ zero matrix and $p \times q$ zero matrix, respectively. i represents a discrete time sample whereas m and n represent the subcarrier and symbol indexes, respectively. The operators $()^*$ and $*$ represent the complex conjugate and convolution of two sequences, respectively. The symbol ϕ denotes an empty set whereas $\cup$ and $\cap$ denote the union and intersection between two sets.

II. System Model

A. Transmit Signal

Consider an uplink FBMC-QAM system in which K UEs transmit data to a single-antenna BS in a grant-free manner. A frequency division multiple access (FDMA) scheme is employed in which each UE transmits its data sporadically on a portion of the M available subcarriers. There is a total of N FBMC-QAM symbols on each subcarrier. At the transmitter of each UE, a stream of information bits $\mathbf{b}$ are encoded to generate a coded bit stream $\mathbf{c}$. The encoded bits are randomly interleaved and mapped onto a QAM constellation to generate the data symbols. Let $d_{m,n}^{(k)} \in \mathcal{M}_k$ denote the QAM modulated data of UE k associated with subcarrier index m and symbol n, where $\mathcal{M}_k$ is the set of subcarriers assigned to UE k and $\mathbb{E}\left[|d_{m,n}^{(k)}|^2\right] = 1$. Here, it is assumed that each subcarrier is allocated to only one UE. Thus, $\cup_{k=1}^{K} \mathcal{M}_k = \{0, 1, \dots, M-1\}$ and $\mathcal{M}_l \cap \mathcal{M}_t = \phi$ for $l \neq t$. Therefore, the discrete time FBMC-QAM transmit signal of UE k can be expressed as

$$s_k[i] = \sum_{m\in\mathcal{M}_k} \sum_{n=0}^{N-1} d_{m,n}^{(k)} g_{m,n}^{(k)}[i] \tag{1}$$

where i represents the sample index and $g_{m,n}^{(k)}[i]$ is the time and frequency shifted version of the the prototype filter impulse response, $g[i]$, given as

$$g_{m,n}^{(k)}[i] = g[i - nM_k/2] e^{j\frac{2\pi mi}{M_k}} \tag{2}$$

where M_k is the number of elements in the set $\mathcal{M}_k$, the sequence $g[i]$ has length $L_k = \kappa \times M_k$ with κ as the overlapping factor. Note that the exponential term in (2) represents the inverse fast Fourier transform (IFFT) operation. As shown in [10], an efficient and low complexity implementation of the prototype filtering in FBMC systems is the poly-phase network (PPN). Adopting the PPN implementation and following the notation in [11], (1) can be rewritten in vector form as

$$\mathbf{s}_k = \mathbf{G}_k \mathbf{d}_k \tag{3}$$

with

$$\mathbf{d}_k = \left[d_{1,1}^{(k)}\ d_{2,1}^{(k)} \dots d_{M_k,1}^{(k)}\ d_{1,2}^{(k)}\ d_{2,2}^{(k)} \dots d_{M_k,N}^{(k)}\right]^T$$

$$\mathbf{G}_k = \left[\mathbf{g}_{1,1}^{(k)}\ \mathbf{g}_{2,1}^{(k)} \dots \mathbf{g}_{M_k,1}^{(k)}\ \mathbf{g}_{1,2}^{(k)}\ \mathbf{g}_{2,2}^{(k)} \dots \mathbf{g}_{M_k,N}^{(k)}\right].$$

Here, $\mathbf{s}_k \in \mathbb{C}^{F_k\times 1}$ is the transmit signal vector of UE k, $\mathbf{d}_k \in \mathbb{C}^{P_k\times 1}$ is the vector of stacked data on all N symbols and M_k subcarriers of UE k, where $F_k = L_k N$ and $P_k = M_k N$. In addition, $\mathbf{g}_{m,n}^{(k)} \in \mathbb{C}^{F_k\times 1}$ is the vector of all samples of $g_{m,n}^{(k)}[i]$ and $\mathbf{G}_k \in \mathbb{C}^{F_k\times P_k}$ is the transmit filter matrix.

B. Received Signal without Timing Offset

In the absence of timing offset (TO), the received signal at the BS from all UEs can be expressed as

$$y[i] = \sum_{k=1}^{K} (s_k[i] * h_k[i]) + z[i] \tag{4}$$

where $h_k[i]$ for $0 \leq i \leq L_{ch} - 1$ is the L_{ch}-tap multipath fading channel between UE k and the BS and $z[i]$ represents the additive white Gaussian noise (AWGN) with zero mean and variance σ_0^2. The vector form of (4) is expressed as

$$\mathbf{y} = \sum_{k=1}^{K} \mathbf{H}_k \mathbf{s}_k + \mathbf{z} \tag{5}$$

where $\mathbf{H}_k \in \mathbb{C}^{F_k\times F_k}$ is the circulant channel matrix of UE k based on $h_k[i]$ and $\mathbf{z} \in \mathbb{C}^{F_k\times 1}$ is the AWGN vector. Note that each element of $\mathbf{H}_k$ is assumed to be an independent and identically distributed (i.i.d) complex Gaussian random variable with zero mean and variance $\sigma_h^2 = \mathbb{E}\left[|h_k[i]|^2\right]$.

C. Received Signal with Timing Offset

Consider the case of grant-free uplink transmission, in which each UE transmits its data asynchronously. In this case, signals from different UEs arrive at the BS with different TO, τ_k. The two cases of TO are illustrated below:

1) Timing error to the right ($\tau_k > 0$): In this case, τ_k samples to the right side of the current FBMC-QAM symbol are replaced with samples from the next symbol. From (1), let the time-domain sequence of the n-th symbol be expressed as $s_{n,k}[i] = \sum_{m\in\mathcal{M}_k} d_{m,n}^{(k)} g_{m,n}^{(k)}[i]$. Thus, the received signal at the BS based on TO to the right can be represented as

$$y_n^r[i] = \sum_{k=1}^{K} \left(x_{n,k}[i + \tau_k] \times R_k[i] + x_{n+1,k}^r[i + \tau_k] \times \bar{R}_k[i]\right) + z[i] \tag{6}$$

where $x_{n,k}[i] = s_{n,k}[i] * h_k[i]$ represents the current symbol and $x_{n+1,k}^r[i + \tau_k]$ is the next symbol. Also, $R_k[i]$ denotes the TO variable with a value of 1 when sample i is selected and 0 when sample i is not selected, i.e.

$$R_k[i] = \begin{cases} 1, & 0 \leq i \leq L_k - \tau_k - 1 \\ 0, & L_k - \tau_k \leq i \leq L_k - 1 \end{cases} \tag{7}$$

and $\bar{R}_k[i]$ is a complement of $R_k[i]$ obtained by swapping 0s and 1s. Substituting (1) into (6) and following the notation in [4], the received signal in (6) can be represented in vector form as

$$\mathbf{y}^r = \sum_{k=1}^{K}\left(\mathbf{R}_k\mathbf{H}_k\mathbf{G}_k\mathbf{d}_k + \bar{\mathbf{R}}_k\mathbf{H}_k\begin{bmatrix}\mathbf{G}_{k,1}\mathbf{d}_k^{next}\\ \mathbf{G}_{k,2}\mathbf{d}_k\end{bmatrix}\right) + \mathbf{z} \quad (8)$$

where $\mathbf{R}_k$ and $\bar{\mathbf{R}}_k \in \mathbb{C}^{F_k\times F_k}$ are the TO matrices, given respectively as

$$\mathbf{R}_k = \begin{bmatrix}\mathbf{0}_{(F_k-\tau_k)\times\tau_k} & \mathbf{I}_{(F_k-\tau_k)}\\ \mathbf{0}_{\tau_k} & \mathbf{0}_{\tau_k\times(F_k-\tau_k)}\end{bmatrix},$$

$$\bar{\mathbf{R}}_k = \begin{bmatrix}\mathbf{0}_{(F_k-\tau_k)\times\tau_k} & \mathbf{0}_{(F_k-\tau_k)}\\ \mathbf{I}_{\tau_k} & \mathbf{0}_{\tau_k\times(F_k-\tau_k)}\end{bmatrix}.$$

Also, $\mathbf{G}_{k,1} \in \mathbb{C}^{(F_k-L_{ch})\times P_k}$ and $\mathbf{G}_{k,2} \in \mathbb{C}^{L_{ch}\times P_k}$ are sub-matrices of $\mathbf{G}_k$ that can be expressed as

$$\mathbf{G}_{k,1} = \mathbf{G}_k(1:(F_k-L_{ch}),:),$$
$$\mathbf{G}_{k,2} = \mathbf{G}_k((F_k-L_{ch}+1):F_k,:).$$

The received signal in (8) can be expanded as

$$\begin{aligned}\mathbf{y}^r &= \sum_{k=1}^{K}((\mathbf{R}_k\mathbf{H}_k\mathbf{G}_k + \bar{\mathbf{R}}_k\mathbf{H}_{k,2}\mathbf{G}_{k,2})\,\mathbf{d}_k + \bar{\mathbf{R}}_k\mathbf{H}_{k,1}\mathbf{G}_{k,1}\mathbf{d}_k^{next}) + \mathbf{z}\\ &= \sum_{k=1}^{K}\left(\mathbf{B}_{k,2}^r\mathbf{d}_k + \mathbf{B}_{k,1}^r\mathbf{d}_k^{next}\right) + \mathbf{z}\end{aligned} \quad (9)$$

where $\mathbf{H}_{k,1}$ and $\mathbf{H}_{k,2}$ are sub-matrices of $\mathbf{H}_k$, i.e. $\mathbf{H}_k = [\mathbf{H}_{k,1}\mathbf{H}_{k,2}]$. Also, $\mathbf{B}_{k,2}^r = \mathbf{R}_k\mathbf{H}_k\mathbf{G}_k + \bar{\mathbf{R}}_k\mathbf{H}_{k,2}\mathbf{G}_{k,2}$ and $\mathbf{B}_{k,1}^r = \bar{\mathbf{R}}_k\mathbf{H}_{k,1}\mathbf{G}_{k,1}$

2) Timing error to the left ($\tau_k < 0$): In this case, τ_k samples to the left side of the current FBMC-QAM symbol are replaced with samples from the previous symbol. In CP-based waveforms, e.g. OFDM and GFDM, the impact of TO to the left can be compensated for using a large enough CP. For a CP duration L_{cp}, only $t = max(L_{ch} - (L_{cp}+\tau_k), 0)$ samples of the previous symbol interfere with the current symbol. However, since FBMC systems do not employ CP, τ_k symbols of the previous symbol will affect the current symbol. Therefore, similar to (6), the received signal at the BS based on TO to the left can be expressed as

$$y_n^l[i] = \sum_{k=1}^{K}\left(x_{n,k}[i+\tau_k]\times R_k[i] + x_{n-1,k}^l[i+\tau_k]\times\bar{R}_k[i]\right) + z[i] \quad (10)$$

where $x_{n-1,k}^l[i+\tau_k]$ is the previous symbol. Similar to (9), the vector form of (10) is represented as

$$\mathbf{y}^l = \sum_{k=1}^{K}\left(\mathbf{R}_k\mathbf{H}_k\mathbf{G}_k\mathbf{d}_k + \bar{\mathbf{R}}_k\mathbf{H}_k\begin{bmatrix}\mathbf{G}_{k,1}\mathbf{d}_k\\ \mathbf{G}_{k,2}\mathbf{d}_k^{prev}\end{bmatrix}\right) + \mathbf{z}. \quad (11)$$

In this case, $\mathbf{R}_k$ and $\bar{\mathbf{R}}_k \in \mathbb{C}^{F_k\times F_k}$ are defined respectively as

$$\mathbf{R}_k = \begin{bmatrix}\mathbf{I}_{(F_k-\tau_k)} & \mathbf{0}_{(F_k-\tau_k)\times\tau_k}\\ \mathbf{0}_{\tau_k\times(F_k-\tau_k)} & \mathbf{0}_{\tau_k}\end{bmatrix},$$

$$\bar{\mathbf{R}}_k = \begin{bmatrix}\mathbf{0}_{(F_k-\tau_k)} & \mathbf{0}_{(F_k-\tau_k)\times\tau_k}\\ \mathbf{0}_{\tau_k\times(F_k-\tau_k)} & \mathbf{I}_{\tau_k}\end{bmatrix}.$$

By expanding the signal in (11), we obtain

$$\begin{aligned}\mathbf{y}^l &= \sum_{k=1}^{K}((\mathbf{R}_k\mathbf{H}_k\mathbf{G}_k + \bar{\mathbf{R}}_k\mathbf{H}_{k,1}\mathbf{G}_{k,1})\,\mathbf{d}_k + \bar{\mathbf{R}}_k\mathbf{H}_{k,2}\mathbf{G}_{k,2}\mathbf{d}_k^{prev})\\ &\quad + \mathbf{z}\\ &= \sum_{k=1}^{K}\left(\mathbf{B}_{k,1}^l\mathbf{d}_k + \mathbf{B}_{k,2}^l\mathbf{d}_k^{prev}\right) + \mathbf{z}\end{aligned} \quad (12)$$

where $\mathbf{B}_{k,1}^l = \mathbf{R}_k\mathbf{H}_k\mathbf{G}_k + \bar{\mathbf{R}}_k\mathbf{H}_{k,1}\mathbf{G}_{k,1}$ and $\mathbf{B}_{k,2}^l = \bar{\mathbf{R}}_k\mathbf{H}_{k,2}\mathbf{G}_{k,2}$.

D. BICM-ID Receiver with Interference Cancellation

In this subsection, description of the proposed receiver is presented for the received signal with and without TO, as shown in Fig. 1. For simplicity of analysis, it is assumed that the channel state information (CSI) is known at the BS.

1) FBMC Demodulation: The received signal is passed through the detection module, shown in Fig. 2. First, the received signal goes through the FBMC-QAM demodulator, which consists of receive filtering and FFT operations. Considering the case of received signal without TO, the frequency domain signal for the k-th UE after filtering and FFT is given as

$$\begin{aligned}\hat{\mathbf{d}}_k &= \mathbf{G}_k^H\mathbf{y}\\ &= \mathbf{G}_k^H\mathbf{H}_k\mathbf{G}_k\mathbf{d}_k + \sum_{u=1,u\neq k}^{K}\mathbf{G}_k^H\mathbf{H}_u\mathbf{G}_u\mathbf{d}_u + \mathbf{G}_k^H\mathbf{z}\end{aligned} \quad (13)$$

Using (1) and (4), the first term in (13) can be expanded as

$$\begin{aligned}\mathbf{G}_k^H\mathbf{H}_k\mathbf{G}_k\mathbf{d}_k &= s_k[i]*h_k[i]\\ &= \sum_{i=-\infty}^{\infty}\sum_{m\in\mathcal{M}_k}\sum_{n=0}^{N-1}d_{m,n}^{(k)}g_{m',n'}^{(k)*}[i]g_{m,n}^{(k)}[i]*h_k[i]\end{aligned} \quad (14)$$

Note that, in OFDM systems the transmit and receive filters are designed to satisfy the orthogonality condition, i.e.

$$\sum_{i=-\infty}^{\infty}g_{m',n'}^{(k)*}[i]g_{m,n}^{(k)}[i] = \delta_{m,m'}\delta_{n,n'} \quad (15)$$

where $\delta_{\{.\}}$ denoted the Kronecker delta function with $\delta_{m,m'} = 1$ if $m = m'$ and $\delta_{m,m'} = 0$ if $m \neq m'$. However, in FBMC-QAM systems, the prototype filters cannot achieve subcarrier orthogonality. Therefore, the expression in (14) can be rewritten as

$$\mathbf{G}_k^H\mathbf{H}_k\mathbf{G}_k\mathbf{d}_k = d_{m',n'}^{(k)}H_k + I_{m',n'}^{(k)}H_k \quad (16)$$

where $H_k = \sum_{i=1}^{L_{ch}}h_k[i]e^{-j\frac{2\pi mi}{M_k}}$ denotes the channel frequency response and $I_{m,n}^{(k)}$ is the InI caused by the lack of subcarrier orthogonality in FBMC-QAM, which is expressed as

$$I_{m',n'}^{(k)} = \sum_{(m',n')\neq(m,n)}d_{m,n}^{(k)}\sum_{i=-\infty}^{\infty}g_{m',n'}^{(k)*}[i]g_{m,n}^{(k)}[i]. \quad (17)$$

Before detection and decoding of the demodulated signal, the effect of the frequency-selective channel is compensated by applying a simple one-tap zero-forcing (ZF) equalizer. Substituting (16) into (13), the estimated data of UE k associated

This article has been accepted for publication in a future issue of this journal, but has not been fully edited. Content may change prior to final publication. Citation information: DOI 10.1109/LCOMM.2021.3085399, IEEE Communications Letters

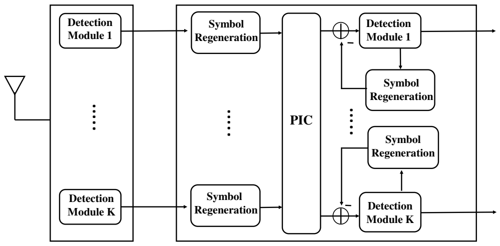

Fig. 1. Proposed BICM-ID receiver with interference cancellation.

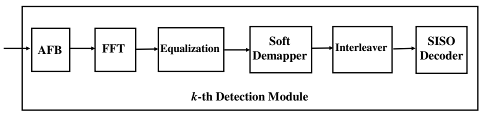

Fig. 2. Block diagram of the Detection Module.

with the m'-th subcarrier of the n'-th symbol after equalization is given by

$$\hat{d}^{(k)}_{m',n'} = d^{(k)}_{m',n'} + I^{(k)}_{m',n'} + \underbrace{\sum_{u=1,u\neq k}^{K} \tilde{\mathbf{H}}_u \mathbf{d}_u}_{\text{MUI}} + \tilde{\mathbf{z}} \tag{18}$$

where $\tilde{\mathbf{H}}_u = \mathbf{H}_k^{-1}\mathbf{G}_k^H \mathbf{H}_u \mathbf{G}_u$ and $\tilde{\mathbf{z}} = \mathbf{H}_k^{-1}\mathbf{G}_k^H \mathbf{z}$.

On the other hand, considering the case with TO, the frequency domain signal of UE k after FBMC-QAM demodulation is given as

$$\begin{aligned}\hat{\mathbf{d}}_k &= \mathbf{G}_k^H \mathbf{y}^J \\ &= \mathbf{G}_k^H \mathbf{B}^J_{k,\nu}\mathbf{d}_k + \mathbf{G}_k^H \mathbf{B}^J_{k,\nu}\mathbf{d}_k^Q \\ &+ \sum_{u=1,u\neq k}^{K}\left(\mathbf{G}_k^H \mathbf{B}^J_{u,\nu}\mathbf{d}_u + \mathbf{G}_k^H \mathbf{B}^J_{u,\nu}\mathbf{d}_u^Q\right) + \tilde{\mathbf{z}}\end{aligned} \tag{19}$$

where $\mathbf{d}_k^Q$ represents the data on the next or previous symbol of UE k, $\{\cdot\}^J$ represents either $\{\cdot\}^r$ or $\{\cdot\}^l$ and ν is either 1 or 2. The second term in (19) represents the TOI. Similar to (13), the first term in (19) consist of the desired signal and InI terms. Thus, after equalization, the detected data signal associated with the m'-th subcarrier of the n'-th symbol can be written as

$$\begin{aligned}\hat{d}^{(k)}_{m',n'} &= d^{(k)}_{m',n'} + I^{(k)}_{m,n} + \underbrace{\tilde{\mathbf{H}}_{k,\nu}\mathbf{d}_k^Q}_{\text{TOI}} + \underbrace{\sum_{u=1,u\neq k}^{K}\left(\tilde{\mathbf{H}}_{u,\nu}\mathbf{d}_u + \tilde{\mathbf{H}}_{u,\nu}\mathbf{d}_u^Q\right)}_{\text{MUI}} \\ &+ \tilde{\mathbf{z}}\end{aligned} \tag{20}$$

where $\tilde{\mathbf{H}}_{k,\nu} = \mathbf{H}_k^{-1}\mathbf{G}_k^H \mathbf{B}^J_{k,\nu}$.

2) Soft Demapper: Using the equalizer output, the soft demapper computes the extrinsic log-likelihood ratios (LLRs) of the b-th bit of the n-th symbol of UE k using sum-product decoding [3]. The extrinsic LLRs, L^e_{Dem}, are deinterleaved and passed to the SISO decoder as *a priori* LLR, L^a_{Dec}.

3) SISO Decoder: The SISO decoder calculates the *a posteriori* LLRs of the coded bits, L^p_{Dec}, after a predefined number of iterations. In this letter, the low-density parity check (LDPC) decoder with an irregular parity-check matrix is considered as the SISO decoder. For the next iteration of the BICM-ID receiver, the extrinsic LLRs, defined as $L^e_{Dec} = L^p_{Dec} - L^a_{Dec}$, are passed to the soft mapper to regenerate the transmitted symbols.

4) Symbol Regeneration: In this step, the transmitted symbols of all UEs are estimated and used for interference cancellation. Specifically, the extrinsic LLRs provided by the SISO decoder are interleaved and passed to a soft mapper as *a priori* information, L^a_{Map}. The output of the soft mapper is FBMC-QAM modulated to obtain the estimates of the transmitted signal from each UE.

5) Interference Cancellation: To remove the InI, TOI and MUI terms from the detected signal, an interference cancellation operation is performed using the regenerated symbols as shown in Fig. 1. The proposed interference cancellation algorithm proceeds as follows:

- In the first iteration, the receiver obtains the soft estimated signals from all K UEs, and removes the MUI terms in (18) and (20) by performing PIC. That is, to decode the signal of UE k, the sum of the signals from all other UEs are subtracted from the received signal of UE k to cancel the MUI.
- In the subsequent iterations, IIC is employed to remove the InI and TOI terms. That is, for each UE the InI and TOI terms are estimated and subtracted from the received signal in multiple decoding iterations.
- When the maximum number of IIC iterations is reached, L^p_{Dec} is used to generate the hard-decision estimates of the transmitted bits, $\hat{\mathbf{b}}$.

A detailed complexity analysis of the proposed receiver is beyond the scope of this letter. Further information and derivation of the complexity analysis of a BICM-ID receiver with interference cancellation is provided in our previous work in [3].

III. Simulation Results

In this section, simulation results are presented to compare the performance of OFDM and FBMC-QAM in an asynchronous uplink FDMA system. For the simulation setup, a 5G NR scenario in which a group of contiguous physical resource blocks (PRB), known as bandwidth part (BWP), is assigned to each UE. Each PRB consists of 12 subcarriers. In this simulation, BWPs made up of 6 PRBs are assigned to each UE. For simplicity, the case of 2 UEs transmitting to the BS is considered in the simulation. The CSI is assumed to be perfectly known at the BS and its powers and delays are defined by the extended vehicular-A (EVA) channel model. For the SISO decoder, an LDPC decoder with irregular parity-check matrix is employed whereas sum-product decoding is used as the demapper. In addition, the PHYDYAS prototype filter with overlapping factor $\kappa = 4$ is used at both the UE and BS. For the synchronous OFDM case, a cyclic prefix of length $L_{cp} = 16$ samples is considered.

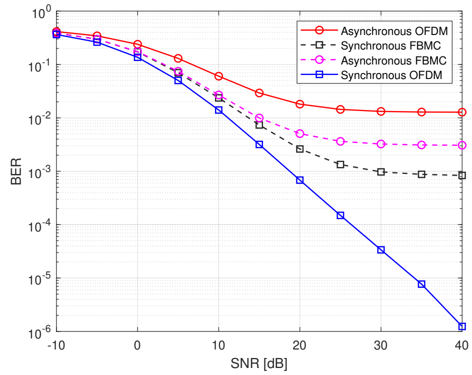

Fig. 3. Average BER performance of OFDM vs FBMC-QAM in Synchronous and Asynchronous multiple access channel

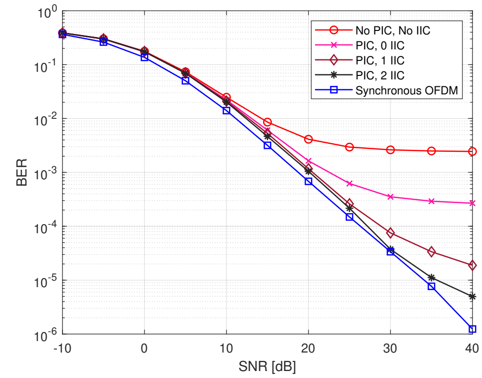

Fig. 4. Average BER performance of proposed BICM-ID receiver with interference cancellation for Asynchronous FBMC-QAM.

First, a comparison of OFDM and FBMC-QAM is presented for two uplink transmission scenarios: (i) the transmission of both UEs are synchronized at the BS, i.e. $\tau_k = 0$ (ii) UE transmissions arrive at the BS with a random number of samples in delay, i.e. $\tau_k > 0$. In the synchronous case, OFDM achieves near optimum BER performance and has no error floor as shown in Fig. 3. This is due to the use of CP and guard band in OFDM, which maintains subcarrier orthogonality and compensates the effect of channel frequency selectivity. On the other hand, an error floor appears at high SNR for FBMC-QAM. This is due to the intrinsic interference caused by the loss of subcarrier orthogonality in FBMC-QAM. As can be seen from Fig. 3, in the asynchronous case FBMC-QAM does not incur a significant performance loss. This is because of the improved frequency localization of FBMC-QAM which reduces its sensitivity to timing errors, without using any CP. In the case of OFDM, asynchronous transmission results in a significant performance loss, especially when the CP is shorter than the number of samples in delay. Thus, FBMC-QAM has the advantage of higher spectral efficiency compared to OFDM since it can combat the effect of timing errors without employing additional resources in terms of CP or guard band.

The BER performance of the proposed BICM-ID receiver with interference cancellation is presented in Fig. 4. As described above, the estimated signals of the two UEs are first used for PIC to remove the MUI term. Then, a fixed number of IIC iterations are performed to eliminate the InI and TOI terms. It can be seen in Fig. 4 that the combination of PIC and IIC is able to remove the InI, TOI and MUI in the proposed FBMC-QAM system. Fig. 4 shows that the error floor can be removed after only 2 IIC iterations.

IV. Conclusion

In this letter, FBMC-QAM has been considered as an alternative to OFDM in an uplink multi-user system in the presence of TO. This is due to the high spectral efficiency and ultra-low OOB emission in FBMC-QAM, which make it suitable for grant-free transmissions. We have derived a general expression for the InI, TOI and MUI and proposed an interference cancellation receiver to eliminate the interference terms. The results show that for the asynchronous case the BER performance of OFDM is significantly degraded compared to the synchronized case. The FBMC-QAM case, on the other hand, shows a robustness against TO with only a small performance loss. It is also shown that the proposed receiver can eliminate the interference terms in multiple receiver iterations. In summary, with a receiver that can effectively remove the interference terms, FBMC-QAM is a convenient alternative to OFDM in uplink transmission due to its robustness to timing errors and high spectral efficiency, which is beneficial for future mMTC applications.

References

[1] B. Lim and Y.-C. Ko, "Multiuser Interference Cancellation for GFDM With Timing and Frequency Offsets," *IEEE Transaction on Communications*, vol. 67, no. 6, pp. 4337–4349, Jun. 2019.

[2] Y. Mostofi and D. C. Cox, "Mathematical analysis of the impact of timing synchronization errors on the performance of an OFDM system," *IEEE Transactions on Communications*, vol. 54, no. 2, pp. 226–230, Feb. 2006.

[3] S. Mahama, Y. J. Harbi, A. G. Burr, and D. Grace, "Design and convergence analysis of an IIC-Based BICM-ID receiver for FBMC-QAM systems," *IEEE Open J. of the Comm. Society*, vol. 1, pp. 563 – 577, May 2020.

[4] B. Lim and Y. Ko, "SIR Analysis of OFDM and GFDM Waveforms With Timing Offset, CFO, and Phase Noise," *IEEE Transactions on Wireless Communications*, vol. 16, no. 10, pp. 6979–6990, Oct. 2017.

[5] S. Mahama, Y. J. Harbi, A. G. Burr, and D. Grace, "A non-orthogonal waveform design with iterative detection and decoding for narrowband IoT applications," in *in Proc. European Conf. Net. Commun.*, 2019, pp. 1–5.

[6] M. Bellanger, D. Le Ruyet, D. Roviras, M. Terré, J. Nossek, L. Baltar, Q. Bai, D. Waldhauser, M. Renfors, T. Ihalainen *et al.*, "FBMC physical layer: a primer," *Phydyas*, vol. 25, no. 4, pp. 7–10, 2010.

[7] P. Singh, H. B. Mishra, A. K. Jagannatham, K. Vasudevan, and L. Hanzo, "Uplink sum-rate and power scaling laws for multi-user massive MIMO-FBMC systems," *IEEE Transactions on Communications*, vol. 68, no. 1, pp. 161–176, Jan. 2020.

[8] D. Gregoratti and X. Mestre, "Uplink FBMC/OQAM-Based Multiple Access Channel: Distortion Analysis Under Strong Frequency Selectivity," *IEEE Transactions on Signal Processing*, vol. 64, no. 16, pp. 4260–4272, Aug. 2016.

[9] S. Mahama, Y. J. Harbi, A. G. Burr, and D. Grace, "Iterative interference cancellation in FBMC-QAM systems," in *Wireless Commun. Net. Conf.*, Apr. 2019, pp. 1–5.

[10] J. Kim, Y. Park, S. Weon, J. Jeong, S. Choi, and D. Hong, "A new filter-bank multicarrier system: The linearly processed FBMC system," *IEEE Trans. Wireless Commun.*, vol. 17, no. 7, pp. 4888–4898, Jul. 2018.

[11] M. Penner, S. Akin, M. Fuhrwerk, and J. Peissig, "Bit error probability for asynchronous channel access with interference cancellation and FBMC," in *2020 IEEE Wireless Communications and Networking Conference (WCNC)*, May 2020, pp. 1–7.